TURBULENCE MODELING OF A SINGLE STREAM CHEVRON NOZZLE FLOW

Rodrigo R. Anjos, rodramos@polo.ufsc.br
Cesar J. Deschamps, deschamps@polo.ufsc.br
POLO Research Laboratories for Emerging Technologies in Cooling and Thermophysics
Federal University of Santa Catarina, Florianópolis, SC, 88040-900, Brazil

Abstract. *Despite considerable advances in LES methods and computational resources, RANS based models are still the only near term approach for prediction of jet noise of industrial interest. The prediction of the acoustic noise generated by a jet flow requires the solution of two problems. The first is the modeling of the source statistics, using the output of a RANS turbulence model to define the amplitude, length and time scales of the sources. The second is the calculation of the propagation of the generated noise to the far field observer. This paper focuses on the first of these problems, by using a non-linear cubic k-ε model. The accuracy of the model is assessed by comparing numerical and experimental data for velocity and Reynolds normal stresses. Although some deficiencies are verified in the predictions, the main features of the flow field are reasonably well captured.*

1. INTRODUCTION

Chevron nozzle is one of the concepts that have been proposed to reduce jet engine noise in commercial aircrafts. Researchers have experimentally demonstrated that certain chevron nozzle configurations can provide nearly 3dB of noise reduction during takeoff with a small thrust loss during cruise. The initial expansion phase of a jet is primarily dependant on the pressure ratio between the reservoir stagnation conditions (p_0) and the ambient pressure, (p_A). As described by Donaldson and Snedeker (1971), a jet may be categorized into one of three types: i) subsonic ($1.0 < p_0/p_A < 1.89$); moderately under-expanded ($2.08 < p_0/p_A < 3.85$) and iii) highly under-expanded ($p_0/p_A > 3.85$). For the subsonic jet, the pressure everywhere in the jet, including at its throat pressure, p_1, will be equal to the ambient pressure, p_A. As depicted in Fig.1, the subsonic jet is characterized by a potential core, surrounded by a mixing region. The radius of this potential core decreases to zero with increasing downstream distance, with the core not existing beyond a certain distance, z_{core}, downstream. Beyond this point, the jet goes through a transitional phase as it continues to expand as the velocity decays, in order to conserve axial momentum, and will eventually reach a fully developed, self-similar, state.

Zaman (1999) carried out an experimental investigation of the spreading characteristics of compressible jets from nozzles of various geometries, covering a jet Mach number range of 0.3 to 2.0. He observed that asymmetric nozzles spread more that circular nozzles only slightly in subsonic conditions, but much more in supersonic conditions. According to Zaman (1999), the presence of tabs provides the largest increase in jet spreading, and eliminates the occurrence of screech in round jets. Chua et al. (2003) carried out an experimental analysis of the effect of tabs on the mixing in an incompressible square jet. Different tab geometries were investigated and the structures formed in different flow conditions were described. They concluded that small tabs can dramatically change the shape of the jet core. Moreover, they found that a two-tab nozzle has a more profound distortion in the jet cross section in relation to the four-tab nozzle.

Bridges and Brown (2004) performed a parametric study of several chevron nozzles called SMC, looking for relationships between chevron geometric parameters, flow characteristics, and far-field noise, in both cold and hot streams at an acoustic Mach number M = 0.9. A stereo PIV was used to acquire mean and turbulent velocities, whereas measurements of far-field acoustics were carried out at a 2.54m radius from 50° to 165° to the jet inlet axis. The geometries were formed by varying chevron count, penetration, length and symmetry. They observed such quantities are correlated with the main flow field parameters of vortex spacing, vortex strength and vorticity distribution. Chevron length was not a major impact on either flow or sound, but penetration was seen to increase noise at high frequency and lower it at low frequency. They verified that asymmetry slightly reduces the impact of the chevron. Although the hot jets differ systematically from the cold one, the overall trends with chevron parameters are the same. Overall, velocity gradients were found to be the most important aspect of noise generation.

Engblom et al. (2004) numerically predicted the flow field and the acoustic noise for a subset of single-stream chevron nozzles tested by Bridges and Brown (2004). Reynolds Averaged Navier-Stokes (RANS) solutions were provided as input to a second code for prediction of the far-field noise distributions. The RANS finite volume flow solver was based in the two equation shear-stress transport (SST) turbulence model (Menter, 1994), whereas Lilley's equations were used to describe the propagation and source of sound. The authors investigated a set of sensitivity cases by varying degrees of chevron inward bend angle relative to the core flow, for both cold and hot exhaust conditions. The RANS model was seen to underpredict the maximum levels of turbulence kinetic energy in the shear layer and to overpredict the core length, although a reasonably agreement with the experimentally measured noise trends was verified for both cold and hot exhaust flow conditions. Both the numerical and experimental results indicate that mixing is enhanced as chevron inward bend angle is increased, resulting in an increase in the peak of turbulence kinetic energy

near the jet exit and an earlier breakdown of the core. Thrust penalties for the chevron configurations were numerically predicted to be minimal.

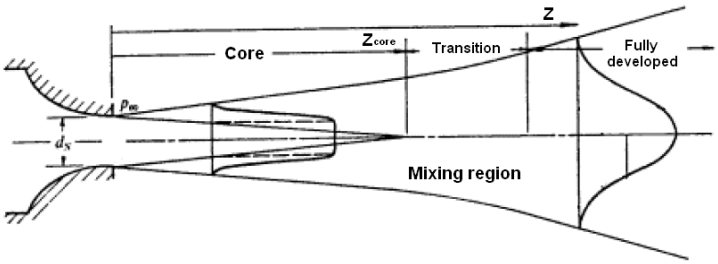

Figure 1. Schematic of a subsonic jet flow from a sonic nozzle; reproduced from Donaldson & Snedeker (1971).

Birch et al. (2006) applied a simple RANS based jet noise prediction procedure to evaluate the acoustic noise for a subsonic condition (M = 0.9). The turbulence model used in the simulations was a modified version of a standard k-ε turbulence model, with slightly different constants being used to model the near and far fields of a jet via an empirical transition function. The authors found that such a model could not fully account for the effect of chevrons on a jet, which appear to affect a jet in two distinct ways. The first effect is that the axial vortices cause a very rapid increase in the width of the mixing layer. This process leads to a local imbalance between the turbulence and the mean flow, a reduction in the turbulence production and an overall reduction in the peak turbulence level, thus contributing to a noise reduction at the lower frequencies. The increase in high frequency noise, often associated with chevron nozzle flows, cannot therefore be explained in terms of a change in the turbulence level. In order to accurately predict the high frequency noise increase, it was found that it was necessary to add a new noise source term that scaled with the strength of the axial vortices. Later, Birch et al. (2007) used a modified version of k-ε turbulence model to evaluate the flow field required by an empirical jet noise prediction model. Results for flow and noise were compared with experimental data for flows that range from single stream jets to more complex coaxial nozzle configurations. They pointed out that a new model needs to be devised in order to account for the effect of chevrons and other advanced noise reduction concepts.

The present paper presents an assessment of the cubic k-ε turbulence model (Craft et al., 1996) to investigate the a single stream chevron nozzle flow for a subsonic condition (M = 0.97), through comparisons between predictions and experimental data for mean velocity and turbulence quantities.

2. PROBLEM FORMULATION

2.1. Flow geometry

In the flow geometry an inlet pipe with a 152.5mm diameter is initially sharply contracted before being rounded out to the final 5° taper and the nozzle end piece (Fig. 2a). The outlet diameter is approximately equal to 51mm. The chevron nozzle geometry SMC006 (Fig. 2b) designed by Bridges and Brown (2004) has been considered in this study. This design has 6 chevrons which penetrate the jet core flow by about 18 degrees. The experimental data was acquired in the Small Hot Jet Acoustic Rig (SHJAR) at NASA Glenn Research Center, by discharging a single-stream air jet from a supply plenum, with stagnation pressure p_0= 178.16kPa and stagnation temperature T_0 = 286.4K into a quiescent ambient with pressure p_A = 97.77kPa and temperature T_A = 280.2K. The Mach number, the static temperature ratio and the Reynolds number of the evaluated cases were, respectively, 0.97, 0.86 and 1.38 x 10^6.

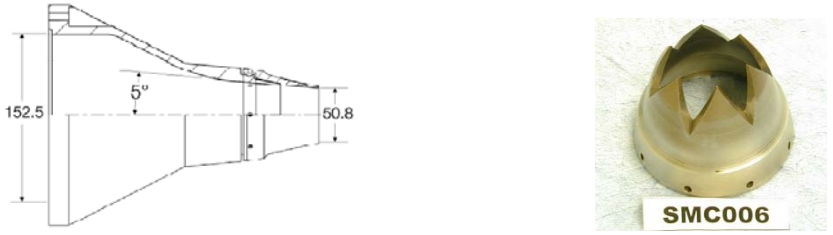

(a) (b)

Figure 2. Nozzle geometry: (a) Overall mounting scheme (dimensions in mm) and (b) chevron nozzle SMC006; reproduced from Bridges and Brown (2004).

2.2. Turbulence modeling

Due to the Mach number associated with the flow situation (M = 0.97), a formulation for compressible flow was adopted, considering the hypothesis of perfect gas. As far as the turbulence model is concerned, the cubic k-ε turbulence model (Craft et al., 1996) was chosen for the simulations.

The non-linear cubic k-ε model solves transport equations for the turbulence kinetic energy (k) and its dissipation rate (ε), with non-linear terms accounting for normal-stress anisotropy, swirl and streamline curvature effects. According to Craft et al. (1996), the following expression for the Reynolds stress anisotropy tensor, a_{ij}, retains terms up to cubic level and satisfies the required symmetry and contraction properties:

$$\begin{aligned} a_{ij} = & -\frac{\nu_t}{k}S_{ij} + c_1\frac{\nu_t}{\tilde{\varepsilon}}\left(S_{ik}S_{jk} - 1/3S_{kl}S_{kl}\delta_{ij}\right) + c_2\frac{\nu_t}{\tilde{\varepsilon}}\left(\Omega_{ik}S_{jk} + \Omega_{jk}S_{ik}\right) + c_3\frac{\nu_t}{\tilde{\varepsilon}}\left(\Omega_{ik}\Omega_{jk} - 1/3\Omega_{kl}\Omega_{kl}\delta_{ij}\right) \\ & + c_4\frac{\nu_t k}{\tilde{\varepsilon}^2}\left(S_{ki}\Omega_{lj} + S_{kj}Q_{li}\right)S_{kl} + c_5\frac{\nu_t k}{\tilde{\varepsilon}^2}\left(\Omega_{il}\Omega_{lm}S_{mj} + S_{il}\Omega_{lm}\Omega_{mj} - \frac{2}{3}S_{lm}\Omega_{mn}\Omega_{nl}S_{ij}\right) \\ & + c_6\frac{\nu_1 k}{\tilde{\varepsilon}^2}S_{ij}S_{kl}S_{kl} + c_7\frac{\nu_t k}{\tilde{\varepsilon}^2}S_{il}\Omega_{kl}\Omega_{kl} \end{aligned} \tag{1}$$

where

$$S_{ij} \equiv \left(\frac{\partial U_i}{\partial x_j} + \frac{\partial U_j}{\partial x_i}\right) \quad ; \quad \Omega_{ij} \equiv \left(\frac{\partial U_i}{\partial x_j} - \frac{\partial U_j}{\partial x_i}\right) - \epsilon_{ijk}\Omega_k \quad ; \quad a_{ij} = \left(\overline{u_i u_j} - 2/3k\delta_{ij}\right)/k \tag{2}$$

and Ω_k is the rotation rate of the coordinate system. The eddy viscosity ν_t ($= c_\mu f_\mu k^2/\tilde{\varepsilon}$) is evaluated in terms of the turbulence kinetic energy k and the so-called isotropic dissipation rate $\tilde{\varepsilon}$ [$= \varepsilon - 2\nu(\partial \mathrm{k}^{1/2}/\,\partial \mathrm{x_j})^2$], which vanishes at the wall (Jones and Launder 1972).

Craft et al. (1996) suggested that the near-wall behavior of turbulence cannot be adequately characterized in terms of a single viscosity-based parameter. Following this argument, they proposed the following expressions for c_μ and f_μ:

$$c_\mu = \frac{0.3}{1 + 0.35\left[\max\left(\tilde{S},\tilde{\Omega}\right)\right]^{3/2}}\left\{1 - \exp\left[\frac{-0.36}{\exp\left(-0.75\,\max\left(\tilde{S},\tilde{\Omega}\right)\right)}\right]\right\} \tag{3}$$

$$f_\mu = 1 - \exp\left[-(R_t/90)^{1/2} - (R_t/400)^2\right] \tag{4}$$

where the Reynolds number of turbulence is defined as $R_t = k^2/\nu\tilde{\varepsilon}$. The coefficients c_1 to c_7 appearing in Eq. (1) are equal to -0.1, 0.1, 0.26, -10 c_μ^2, 0, -5 c_μ^2, 5 c_μ^2, respectively. Besides the indicated role of the stress and vorticity tensors in Eq. (1), the following dimensionless strain and vorticity invariants have been adopted in Eq. (3):

$$\tilde{S} = k/\tilde{\varepsilon}\sqrt{1/2S_{ij}S_{ij}} \quad ; \quad \tilde{\Omega} = k/\tilde{\varepsilon}\sqrt{1/2\Omega_{ij}\Omega_{ij}} \tag{5}$$

The turbulent kinetic energy k and its dissipation rate are obtained from the following transport equations:

$$\frac{Dk}{Dt} = P_k - \varepsilon + \frac{\partial}{\partial x_j}\left[(\nu + \nu_t/\sigma_k)\frac{\partial k}{\partial x_j}\right] \tag{6}$$

$$\frac{D\bar{\varepsilon}}{Dt} = c_{\varepsilon 1}\frac{\tilde{\varepsilon}}{k}P_k - c_{\varepsilon 2}\frac{\tilde{\varepsilon}^2}{k} + E + Y_c + \frac{\partial}{\partial x_j}\left[(\nu + \nu_t/\sigma_\varepsilon)\frac{\partial \tilde{\varepsilon}}{\partial x_j}\right] \tag{7}$$

where

$$P_k = -\overline{u_i u_j}\frac{\partial U_i}{\partial x_j} \quad \text{and} \quad \varepsilon = \tilde{\varepsilon} + 2\nu\left(\frac{\partial\sqrt{k}}{\partial x_j}\right)^2 \tag{8}$$

The Prandtl numbers for turbulent transport in the k and ε equations are empirical constants; σ_k =1.0 and σ_ε =1.3. The parameter $c_{\varepsilon 1}$ is equal to 1.44, whereas $c_{\varepsilon 2}$ is expressed as $c_{\varepsilon 2} = 1.92 - [1 - 0.3\exp(-R_t)^2]$.

The near-wall source term E in Eq. (7) assumes a modified form of the original proposal put forward by Launder and Sharma (1974):

$$E = 0.0022\frac{\bar{S}\nu_t k^2}{\tilde{\varepsilon}}\left(\frac{\partial^2 U_i}{\partial x_j \partial x_k}\right)^2 \qquad \text{for} \quad R_t \leq 250 \tag{9}$$

With the aim of reducing the turbulence length scales predicted by the linear k-ε model in separated flow regions, Yap (1987) proposed a length-scale correction Y_c, which is retained in the cubic model and written as:

$$Y_c = \max\left[0.83\frac{\tilde{\varepsilon}^2}{k}\left(\frac{k^{3/2}}{2.5\tilde{\varepsilon}y} - 1\right)\left(\frac{k^{3/2}}{2.5\tilde{\varepsilon}y}\right)^2, 0\right] \tag{10}$$

where y is the distance to the wall.

3. NUMERICAL SOLUTION PROCEDURE

Numerical simulations were carried out with the commercial code CFD^{++} (Metacomp, 2005). The solution procedure available in the code offers second-order accuracy and the ability to handle multi-block grids. The length of the domain corresponds to approximately 49 diameters. For the inflow condition, velocity, pressure and temperature were determined from isentropic relations for ideal gas, whereas turbulence was characterized by an intensity of 1% and a length scale equal to the nozzle diameter. A standard two-layer wall-function was employed to bridge the nozzle wall surface and the fully-turbulent region. For the remaining boundaries, a free stream static pressure was adopted. Accordingly, when the flow enters the solution domain, a reservoir boundary condition is imposed with negligible turbulence. On the other hand, when the flow leaves the flow domain, a back-pressure is imposed and all the other quantities are extrapolated from the solution domain interior. Convergence of the iterative procedure was verified by monitoring variations in numerical results for the centerline axial velocity, temperature and turbulent kinetic energy as the value for the convergence criterion was progressively made stricter.

A very important aspect in numerical simulations is the assessment of truncation errors present in the solution, which is possible through tests of grid refinement. In the present work, this objective was reached by simulating an axisymmetric jet with three different levels of grid refinement. Initially a structured grid was developed with 25,313 quadrilateral elements (M002). Based on the grid M002, two additional grids were constructed: grid M004 with 49,744 and grid M006 with 100,691 elements. Results for velocity along the jet axis obtained with the coarse (M002), medium (M004) and fine (M006) grids showed insignificant differences, providing evidence of grid independence.

Three-dimensional grids for the SMC006 nozzle were then constructed based on the results of the aforementioned truncation tests. Figures 3 and 4 show grid slices for longitudinal and cross-section planes, as well the grid on the chevron nozzle surface. The resulting grid consisted of approximately 2.6 million cells, with the grid refinement adjacent to the solid surfaces returning a y+ value between 15 and 100.

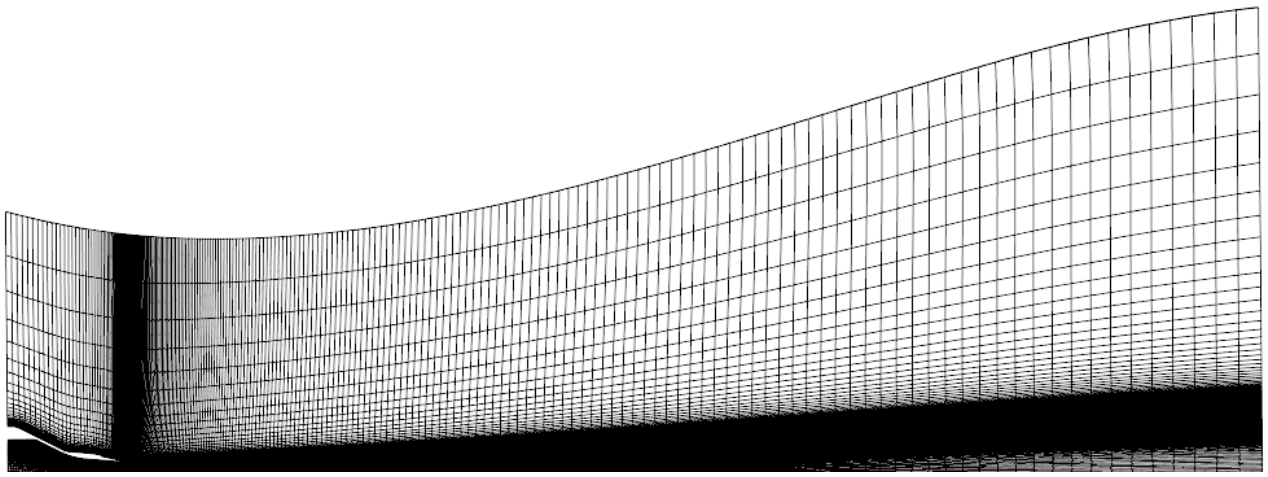

Figure 3. Longitudinal grid plane.

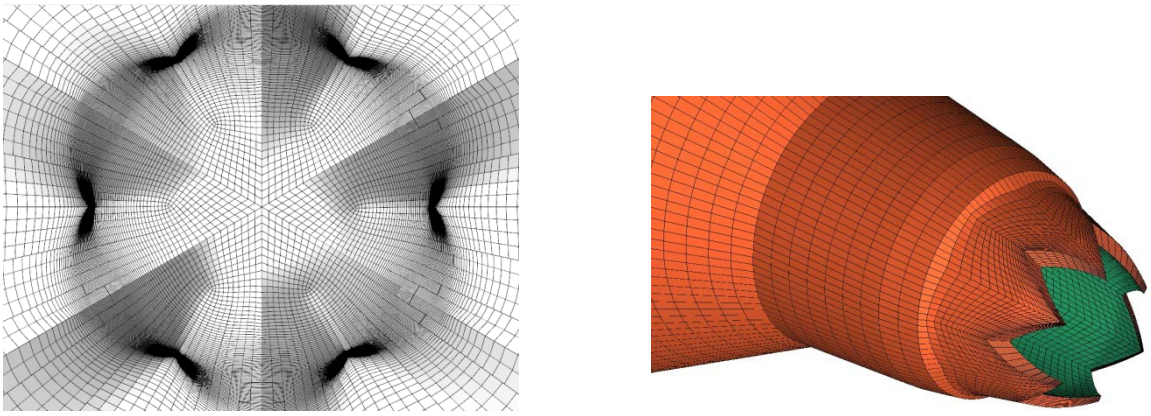

(a) Cross-section plane next to nozzle exit. (b) Chevron nozzle surface.

Figure 4. Computational grid.

4. RESULTS

Figure 5 presents results for contours of Mach number along two longitudinal slices, one from tip to tip (Fig. 5a) and the other from valley to valley (Fig. 5b) of the chevron petal, and three cross section slices at downstream (X/Dj = 0.1, 5 and 10), where X is the axial distance starting from the chevron trailing edge and Dj is the nominal core diameter of 2" (≅ 51mm). The results clearly show the shear layer and mixing along the jet. Moreover, it is possible to verify that the mixing layer growth is considerably different in both longitudinal slices. As the shear layers grows downstream, the elongated peak regions from opposing sides of the chevrons gradually merge, with the jet showing azimuthal uniformity at X/D=10.

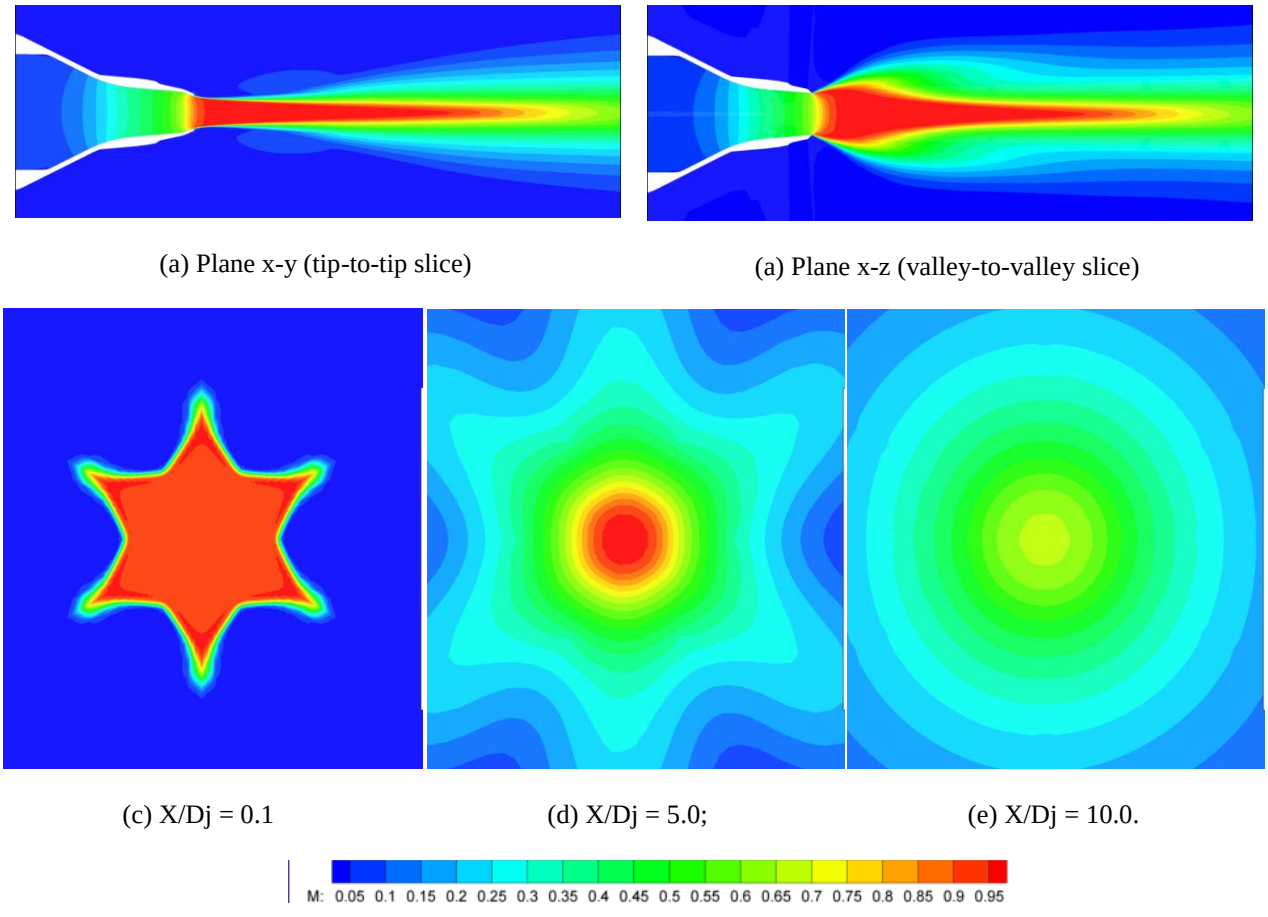

(a) Plane x-y (tip-to-tip slice) (a) Plane x-z (valley-to-valley slice)

(c) X/Dj = 0.1 (d) X/Dj = 5.0; (e) X/Dj = 10.0.

Figure 5. Results for Mach number contours along two longitudinal planes and three cross sections.

An initial assessment of the numerical model was made possible through comparisons between prediction and experimental data for velocity along the centerline (Fig. 6). As can be seen, the numerical model over predicts the length of the core region. In fact, Birch et al. (2003) observed that the standard k-ε model over predicts the core length by about 15% for axisymmetric jets, whereas Engblom (2004) observed the same anomaly with the SST model. Therefore, the non-linear k-ε model adopted in the present study shows a similar behavior. In fact, this is a well known deficiency of the RANS models, which is usually remediated by introducing ad-hoc adjustments such as those proposed by Pope (1978) and (Bardina et al., 1983).

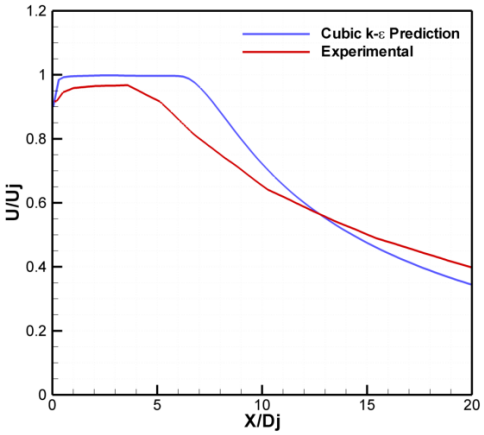

Figure 6. Experimental and numerical results for velocity along the jet center line.

Figures 7 and 8 illustrate numerical and experimental results for profiles of Reynolds normal stresses ($\overline{uu}, \overline{vv}$ and $\overline{ww}$) at two cross sections X/Dj = 5 and 10, respectively, considering slices from tip to tip and from valley to valley of the chevron petal. The normal stress distributions agree reasonably well with the experimental data, despite an under prediction of stress levels in the jet centerline for X/Dj = 5, which is related to over prediction of the potential core length. Predicted normal stress levels at X/Dj = 5 and 10 are greater than those indicated in the measurements, which will be reflected in the turbulence kinetic energy. It is interesting to note that, notwithstanding such discrepancies, the normal stress component $\overline{uu}$ returned by the model is fairly close to the experimental data for all cross sections.

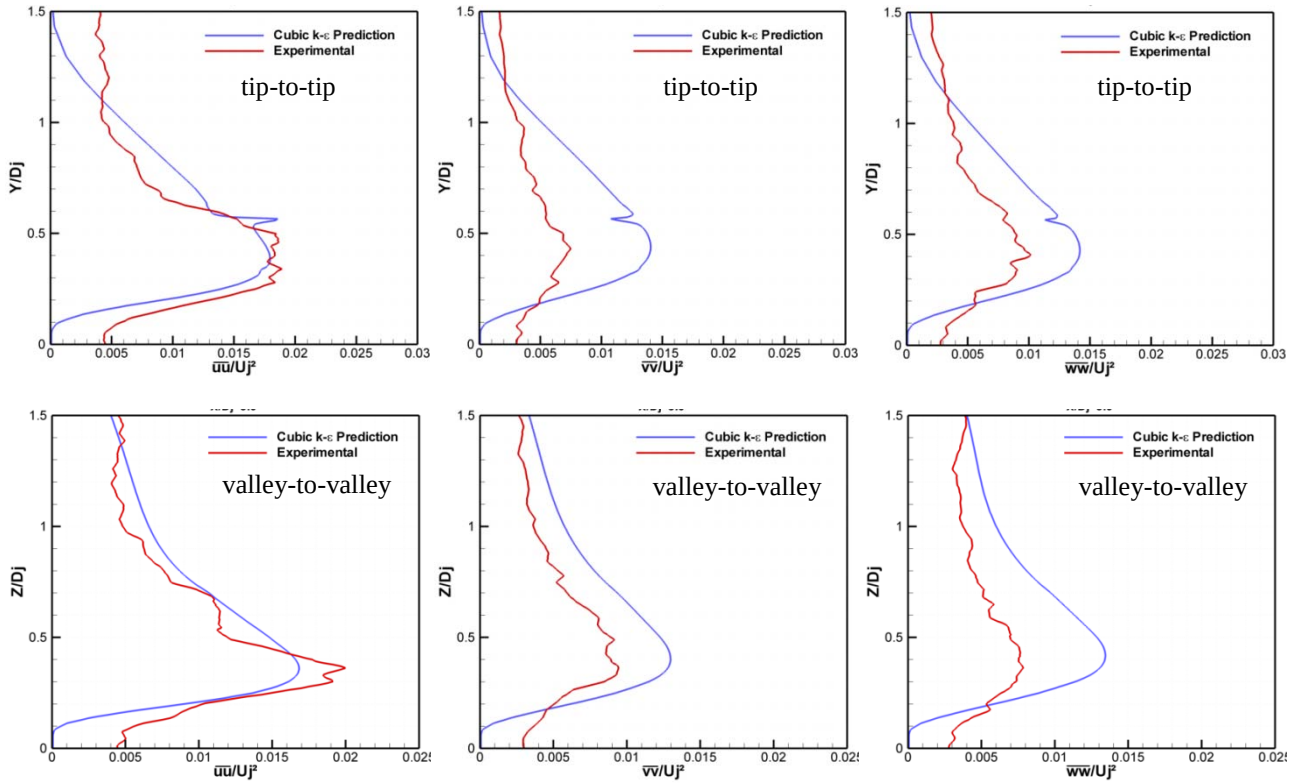

Figure 7. Experimental and numerical results for Reynolds normal stresses; X/Dj = 5.0.

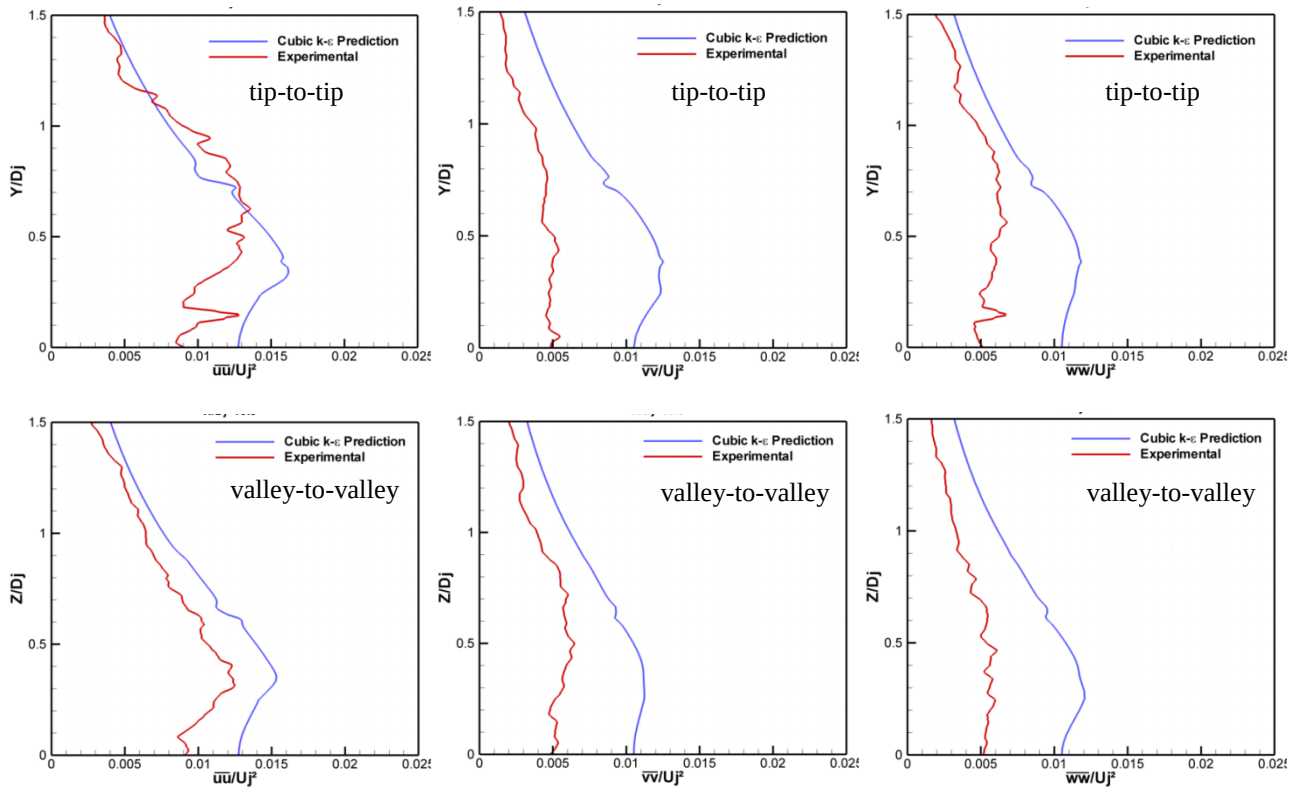

Figure 8. Experimental and numerical results for Reynolds normal stresses; X/Dj = 10.0.

Unlike linear eddy-viscosity models, the cubic *k-ε* model was developed to give a meaningful separation between the normal stress components. However, the difference between the fluctuating velocities found in the present simulation is not as large as is verified in the experimental data, particularly when $\overline{vv}$ and $\overline{ww}$ are compared to $\overline{uu}$. This is a deficiency that may have an impact on noise prediction. Therefore, the adoption of a Reynolds stress model (RSM) in place of the turbulence viscosity concept is a worthwhile test for future studies, since stress-transport models were developed to offer a more reliable way of handling complex strain fields.

Comparisons between predictions and experimental data for turbulent kinetic energy, *k*, at two longitudinal positions (X/Dj = 5 and 10) are shown in Fig. 9, for slices from tip to tip and from valley to valley of the chevron petal. As expected, the level of agreement between both results is in line with that observed for normal Reynolds stresses (Figs. 7 and 8). Consequently, there is an under prediction of *k* in the jet centerline at X/Dj = 5 and a considerable overprediction at X/Dj = 10. It should be noticed that Reynolds stresses, $\overline{u_i u_j}$, and the dissipation rate, ε, provided by the RANS solution are used to construct spatially and temporally correlated velocity fluctuations that are needed in some noise prediction methods. However, the accuracy requirement for such quantities within the framework of these approaches is not yet clear and will be assessed through extensive tests in future study.

5. CONCLUSIONS

The prediction of the acoustic noise generated by jet flows requires the numerical modeling of the source statistics, using the output of a turbulence model to define the amplitude, length and time scales of the sources. The present paper considered the turbulence modeling of a single-stream chevron nozzle flow, by using a non-linear cubic k-ε model. The accuracy of the model was assessed through comparisons between numerical and experimental results for velocity, Reynolds normal stresses and turbulent kinetic energy. Although some deficiencies were verified in the predictions, the main features of the flow field were reasonably well captured. In fact, there have been several studies focused on applying Reynolds Averaged Navier-Stokes (RANS) equations to predict chevron nozzle flows, with particular attention to mixing and development of the jet. The results have shown that simulation methods based on RANS are not accurate because of turbulence modeling shortcomings. Since success in the predictions of acoustic noise generated by chevron nozzles is directly connected to the degree of accuracy with which the flow field is estimate, it is necessary to develop reliable simulation methods so as to correctly predict the effect of geometric modifications on the flow and, as a consequence, on the acoustic field.

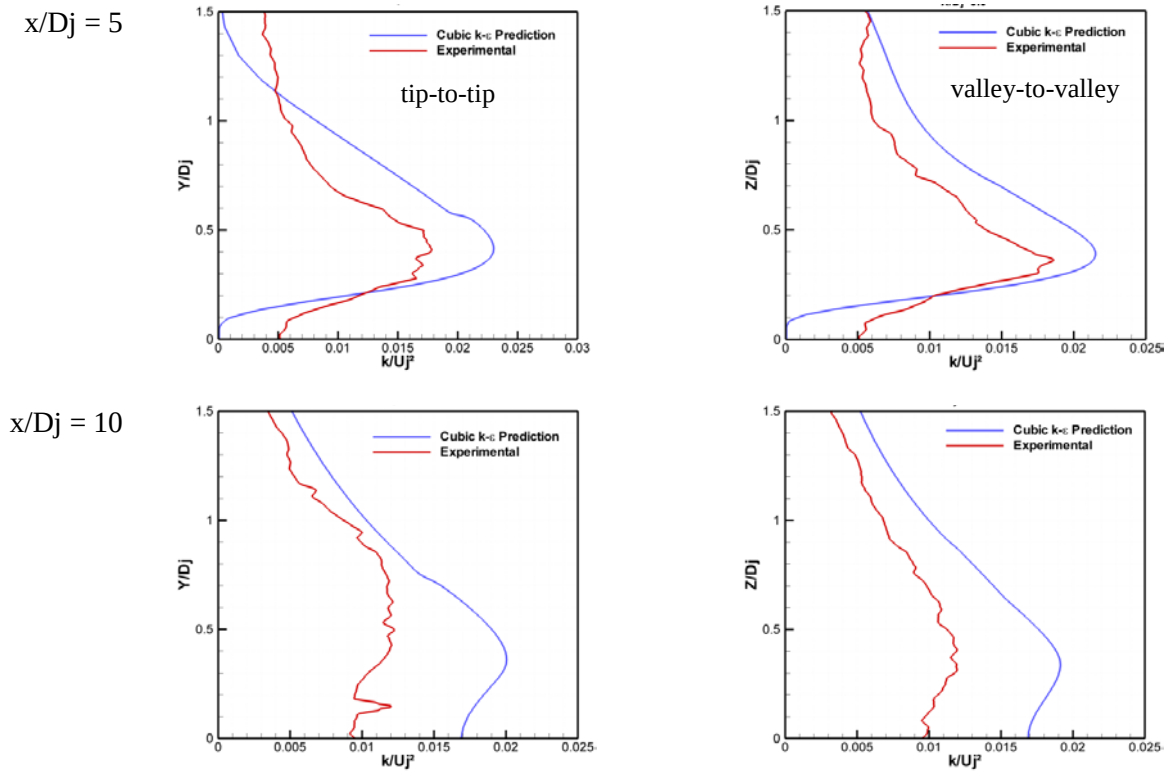

Figure 9. Experimental and numerical results for turbulent kinetic energy.

6. ACKNOWLEDGEMENTS

The study reported herein was funded by EMBRAER, FAPESP and CNPq under National Grant No. 573581/2008-8 (National Institute of Science and Technology in Refrigeration and Thermophysics). The authors gratefully acknowledge James Bridges (NASA Glenn Research Center) for providing the experimental data associated with the chevron nozzle SMC006.

7. REFERENCES

Bardina, J., Ferziger, J., and Reynolds, W.C., 1983, “Improved turbulence models based on large-eddy simulation of homogeneous, incompressible, turbulent flows”. Mechanical Engineering Department TF-19, Stanford University.

Birch, S.F., Lyubimov, D.A., Secundov, A.N. and Yakubovsky, K.Y., 2003, “Numerical Modeling Requirements for Coaxial and Chevron Nozzle Flows”, Proc. 9th AIAA/CEAS Aeroacoustics Conference, Hilton Head, United States, Paper AIAA 2003-3287.

Birch, S.F., Lyubimov, D.A., Maslov, V.P., Secundov, A.N. and Yakubovsky, K.Y., 2007, “A RANS based Jet Noise Prediction Procedure”, Proc. 13th AIAA/CEAS Aeroacoustics Conference, Rome, Italy, Paper AIAA 2007-3727.

Birch, S.F., Lyubimov, D.A., Maslov, V.P., Secundov, A.N., 2006, “Noise Prediction for Chevron Nozzle Flows”, 12th AIAA/CEAS Aeroacoustics Conference, Cambridge, United States, Paper AIAA 2006-2600.

Bridges, J. and Brown, C.A., 2004, “Parametric testing of chevrons on single flow hot jets”, Proc. 10th AIAA/CEAS Aeroacoustics Conference, Manchester, UK, paper AIAA-2004-2824

Chua, L.P., Yu, S.C.M. and Wang, X.K., 2003, “Flow visualization and measurements of a square jet with mixing tabs”, Experimental Thermal and Fluid Science, Vol.27, pp. 731-744.

Craft, T.J., Launder, B.E. and Suga, K., 1996, “Development and application of a cubic eddy-viscosity model of turbulence”, Int. J. Heat and Fluid Flow, Vol.17, pp. 332-340.

Donaldson, C.D. and Snedeker, R.S., 1971, "A study of free jet impingement, part 1", J. Fluid Mechanics, Vol.45, pp. 281-319.

Engblom, W.A., Khavaran, A., and Bridges, J., 2004, “Numerical Prediction of Chevron Nozzle Noise Reduction Using WIND-MGBK Methodology”, Proc. 10th AIAA/CEAS Aeroacoustics Conference, Manchester, UK, Paper AIAA 2004-2979.

Jones, W.P. and Launder, B.E., 1972, “The prediction of laminarization with a two-equation model of turbulence, Int. J. Heat Mass Transfer”, Vol.15, pp. 301-314.

Launder, B.E. and Sharma, B.I., 1974, "Application of the Energy-Dissipation Model of Turbulence to the Calculation of Flow Near a Spinning Disc", Letters in Heat and Mass Transfer, Vol. 1, No. 2, pp. 131-138.

Menter, F.R., 1994, “Two-Equation Eddy-Viscosity Turbulence Models for Engineering Applications”. AIAA Journal, Vol.32, No. 8, pp. 1598–1605.

Metacomp Technologies, 2005, “User´s Manual”.

Pope, S.B., 1978, “An explanation of the turbulent round-jet/plane-jet anomaly”. AIAA J. 16, 279-281.

Zaman, K.B.M.Q., 1999, “Spreading characteristics of compressible jets from nozzles of various geometries”, Journal of Fluid Mechanics, Vol. 383, pp. 197-228.

8. RESPONSIBILITY NOTICE

The authors are the only responsible for the printed material included in this paper.